International Journal of Advanced Structural Engineering, Vol. 3, No. 2, Pages 133-151, December 2011

Published online December 2011 at (http://journals.azad.ac.ir/IJASE)

NONLINEAR ANALYSIS OF REINFORCED CONCRETE COLUMNS WITH FIBER REINFORCED POLYMER BARS

Ehab M. Lotfy[1]
Faculty of Engineering, Suez Canal University, Ismaelia, Egypt

Received 7 February 2011
Revised 22 September 2011
Accepted 1 October 2011

In this paper, the results of an analytical investigation on the behavior of RC columns reinforced with fiber reinforced polymer bars FRP are presented and discussed. Nonlinear finite element analysis on 10-column specimens was achieved by using ANSYS software. The nonlinear finite element analysis program ANSYS is utilised owing to its capabilities to predict either the response of reinforced concrete columns in the post-elastic range or the ultimate strength of a reinforced concrete columns reinforced by FRP bars. An extensive set of parameters is investigated including different main reinforcement ratios, main reinforcement types (GFRP, Steel), the transverse reinforcement ratios, and the characteristic compressive strength of concrete. A comparison between the experimental results and those predicted by the existing models are presented. Results and conclusions may be useful for designers, have been raised, and represented.

Keywords: inelastic finite element analysis, reinforced concrete columns, fiber polymer bars, ANSYS, compressive behavior

1. Introduction

Fiber reinforced polymer (FRP) is increasingly used for reinforcing new structures, and strengthening existing structures. FRP composites, in the form of sheets, cables, rods, and plates, have proven to be a cost-effective alternative to steel reinforcements because of their low weight to strength ratio, corrosion resistance, and flexibility. The most common types of FRP are aramid, glass, and carbon; AFRP, GFRP, and CFRP, respectively.

[1] Lecturer

Correspondence to: Dr. Ehab M. Lotfy, Faculty of Engineering, Suez Canal University, , 10 Elsalam St., Zagazig, Ismaelia, Egypt, E-mail: ehablotfy2000@yahoo.com

Unfortunately, there was lack of data about using FRP as reinforcement; lack of a comprehensive database on FRP materials makes it difficult for the practicing civil engineer and designer to use FRP composites on a routine basis, although a number of reviews have been published recently related to durability and test methods.

The focus of each has been to summarize the state of knowledge in general without emphasizing or attempting to prioritize critical areas in which needs are the greatest for collection, assimilation, and dissemination of data (Karbhari et al., 2003).

There are many bridge structures all over the world as applications of structures with FRP reinforcement for example:

1- In China; there are now eight GFRP bridges in China. These bridges were generally constructed by hand lay-up of glass fibers in a polyester resin using a honeycomb form of deck structure, as the Miyun Bridge, the Xianyyong bridge, and Hulan River Bridge.

2- In Germany; the Lünensche Gasse pedestrian bridge, the Ulenbergstrasse Bridge, and the Schiessbergstrasse Bridge.

3- In Japan; the Shinmiya Highway Bridge, the Bachi-Minami-Bashir highway bridge, the Nagatsugawa pedestrian Bridge, Tochigi Prefecture Bridge, and Ibaraki Prefecture Bridge.

4- In Canada; the Beddigton Trail Bridge, the Headingley Bridge, Wotton Bridge, and Magog Bridge

5- In the United States: the McKinleyville Bridge, and the Morristown Bridge (Nicolas and Rajan, 2003; Halcrow et al., 1996; Ou, 2003; El-Salakawy, 2003).

ACI Committee 440 contained design provisions for flexure and shear, the guide excludes any provisions for the analysis and design of concrete compression members reinforced with FRP bars. FRP bars were not recommended by ACI Committee 440 (1996, 2003) for use as compression reinforcement, in part because the direct effect of compression reinforcement on the strength of concrete members is frequently small and; therefore, often ignored. Additionally, the compression properties of FRP bars are often difficult to predict due to the lack of stability of individual fibers in a bar. Therefore, this complicates testing and can produce inaccurate measurements of compression properties (ACI, 2006; Choo et al., 2006).

So, this study aims to study the behavior of reinforced concrete columns with GFRP. The results and observations presented in this paper are useful to practicing engineers who must predict the enhanced compressive strength of concrete columns reinforced with GFRP bars.

2. Objectives and Scope

The main objectives of this study could be summarized in the following points:

- ♦ Examining the compressive behavior of reinforced concrete columns with GFRP-bars.
- ♦ Comparing this behavior with reinforced concrete columns with steel rebar.

Finite element models were developed to simulate the behavior of reinforced concrete columns with GFRP-bars from linear through nonlinear response using the ANSYS program.

3. Experimental Program

The experimental program included testing of GFRP and steel RC columns under pure axial load, the specimens had square cross-section with a 250mm side, and length of 1250 mm, the test matrix is shown in Table 1, from C1 to C8

The analysis carried out is conducted on 10-RC columns; the parameters of study were the main reinforcement ratios, and types, the transverse reinforcement ratios, and the characteristic compressive strength of concrete. Finally, conclusions from the current research and recommendations for future studies are presented.

Table 1. Details of Tested Columns Specimens

Group No.	Col. No.	Dim (mm) Dim	Dim (mm) L	f_{cu} (N/mm^2)	Reinf.	Reinf. Ratio (%)	Steel Stirrups in the Col. Ends	Notes
1	C1	250*250	1250	25	4#12mm	0.723	(ø 6mm@120mm)	1-GFRP reinf 2-Stirrups shape (A)
	C2			25	6#12mm	1.08	(ø 6mm@120mm)	1-GFRP reinf 2-Stirrups shape (A)
	C3			25	8#12mm	1.45	(ø 6mm@120mm)	1-GFRP reinf 2-Stirrups shape (A)
2	C4			25	4#12mm	0.723	(ø 6mm@120mm)	1-Steel reinf 2-Stirrups shape (A)
3	C5			30	4#12mm	0.723	(ø 6mm@120mm)	1-GFRP reinf 2-Stirrups shape (A)
	C6			35	4#12mm	0.723	(ø 6mm@120mm)	1-GFRP reinf 2-Stirrups shape (A)
4	C7			25	4#12mm	0.723	(ø 6mm@60mm)	1-GFRP reinf 2-Stirrups shape (B)
	C8			25	4#12mm	0.723	(ø 6mm@60mm)	1-GFRP reinf 2- Stirrups shape (C)
5	C9			25	4#16mm	1.286	(ø 6mm@120mm)	1-GFRP reinf 2-Stirrups shape (A)
	C10			25	4#18mm	1.628	(ø 6mm@120mm)	1-GFRP reinf 2-Stirrups shape (A)

4. Numerical Finite Element

4.1. Basic Fundamentals of the FE Method

The basic governing Equations for two dimensions elasto-plastic FEM have been well documented (Zienkiewics, 1967), and are briefly reviewed here.

I. Strain - displacement of an element

$$[d\varepsilon]=[B][dU] \tag{1}$$

Where: [B] is the strain-displacement transformation matrix. The matrix [B] is a function of both the location and geometry of the suggested element, it represents the shape factor. The matrix [B] for a triangle element having nodal points 1, 2 and 3 is given by:

$$[B]=\frac{1}{2\Delta}\begin{bmatrix} y_2-y_3 & 0 & y_3-y_1 & 0 & y_1-y_2 & 0 \\ 0 & x_3-x_2 & 0 & x_1-x_3 & 0 & x_2-x_1 \\ x_3-x_2 & y_2-y_3 & x_1-x_3 & y_3-y_1 & x_2-x_1 & y_1-y_2 \end{bmatrix} \tag{2}$$

Where xi and yi represent the coordinates of the node and Δ represents the area of the triangular element, i.e.

$$2\Delta = det\begin{vmatrix} 1 & x_1 & y_1 \\ 1 & x_2 & y_2 \\ 1 & x_3 & y_3 \end{vmatrix} \tag{3}$$

II. Stress - strain relation or field Equation

$$[d\sigma] = [D]\,[d\varepsilon] \tag{4}$$

Here, [D] is the stress- strain transformation matrix. For elastic elements the matrix from the Hooke's law leads to $[D] = [D^e]$. For plastic elements, the Prandtl-Reuss stress-strain relations together with differential forms of the von Mises yield criterion as a plastic potential leads to:

$$[D] = [D^p] \tag{5}$$

The elastic matrix, $[D^e]$, is given by elastic properties of the material whereas the plastic matrix, $[D^e]$, is a function of the material properties in the plastic regime and the stress-strain elevation. Obviously, for two-dimensional analysis $[D^e]$ and $[D^p]$ depend on the stress-strain state, i.e. plane stress versus plane strain.

The plastic matrix, $[D^p]$, depends on the elastic-plastic properties of the material and the stress elevation. Comparing $[D^e]$ and $[D^p]$, it can be seen that the diagonal elements of $[D^p]$ are definitely less than the corresponding diagonal elements in $[D^e]$. This amounts to an apparent (crease in stiffness or rigidity due to plastic yielding. Therefore, the plastic action reduces the strength of the material.

III. Element stiffness matrix $[K^e]$

$$[K^e] = \iiint [B]^T [D][B] dv \tag{6}$$

The transpose matrix of [B] is $[B]^T$. In the case of well-known triangular elements [k] is represented by;

$$[K] = [B]^T [D][B] V \tag{7}$$

The element volume is V and for a two-dimensional body equals the area of the element, Δ, multiplied by its thickness, t.

IV. The overall stiffness matrix [K]

The stiffness matrixes $[K^e]$ of the elements are assembled to form the matrix [K] of the whole domain. The overall stiffness matrix relates the nodal load increment [dP] to the nodal displacement increment [du] and can be written as:

$$[dP] = [K] [du] \tag{8}$$

This stiffness relation forms a set of simultaneous algebraic Equations in terms of the nodal displacement, nodal forces, and the stiffness of the whole domain. After imposing appropriate boundary conditions, the nodal displacements are estimated, and consequently the stress strain field for each element can be calculated.

5. Finite Element Modelling

5.1. Geometry

The details of the tested columns were shown in Figure 1. Analyses were carried out on 10-columnspecimens, where all columns had square cross-section with a 250mm side and length of

1250mm. Analyzed columns had main reinforcement with GFRP bars 4#12mm, 6#12mm, and 8#12mm, 4#16mm, and 4#18mm, and with steel bars 4#12mm.

The transverse reinforcement was ϕ6 mm closed stirrups spread in 120mm, and 60mm, and characteristic strength of concrete columns 25, 30, and 35 N/mm^2. The analyzed columns were divided into four different groups as shown in Table 1.

In this study, the perfect bond between concrete and reinforced bars was assumed. To provide the perfect bond, the link element for the reinforcing bars was connected between the nodes of each adjacent concrete solid element, so the two materials shared the same nodes.

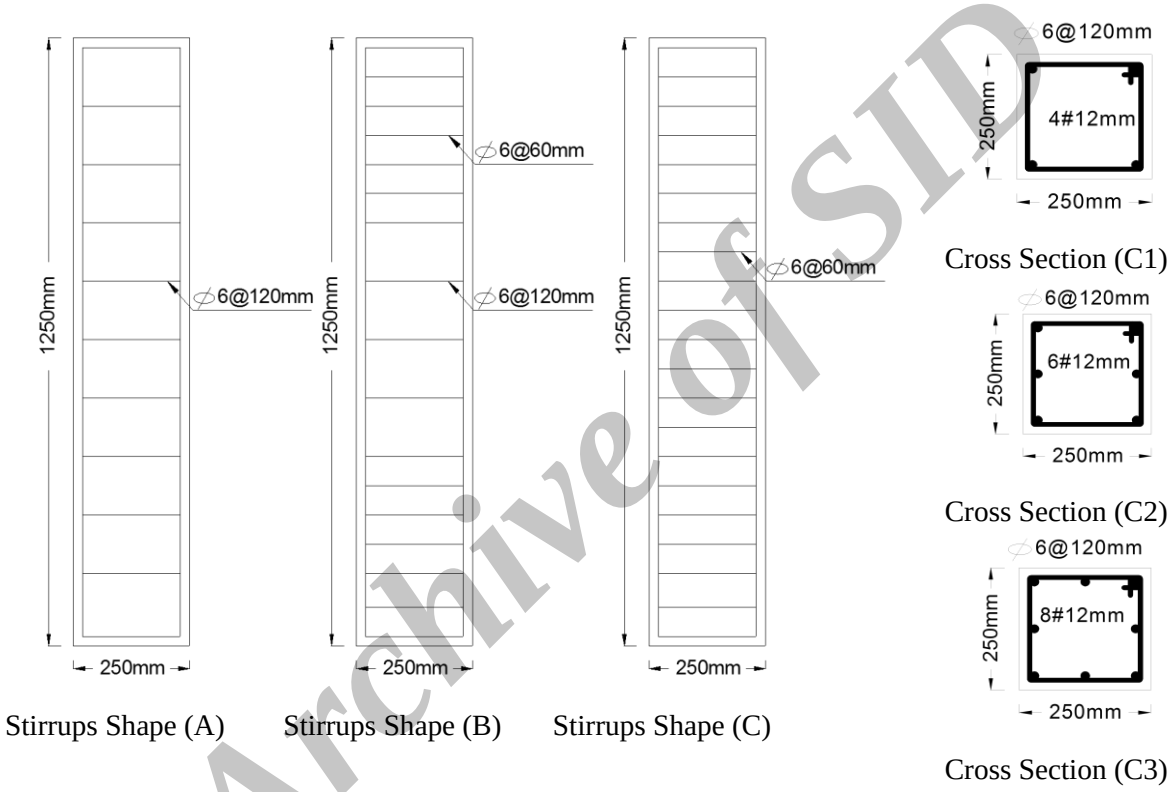

Figure 1. Details of reinforcement of tested columns

6. Element Types and Material Properties

Extensive inelastic finite element analyses using the ANSYS program are carried out to study the behavior of the tested columns. Two types of elements are employed to model the columns. An eight-node solid element, solid65, was used to model the concrete. The solid element has eight nodes with three degrees of freedom at each node, translation in the nodal x, y, and z directions. The used element is capable of plastic deformation, cracking in three orthogonal directions, and crushing. A link8 element was used to model the reinforcement polymer bar; two nodes are required for this element. Each node has three degrees of freedom, translation in the nodal x, y,

and z directions. The element is also capable of plastic deformation (ANSYS). The finite element mesh used in the analysis is shown in Figure 2.

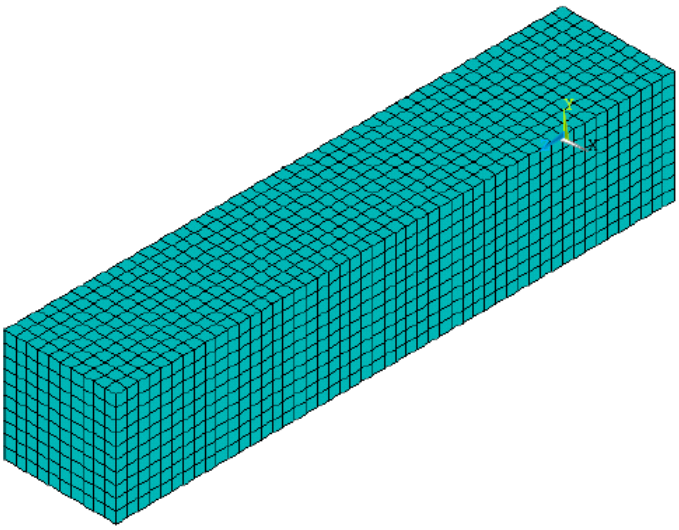

Figure 2. Finite element mesh for a typical column model

Normal weight concrete was used in the fabricated tested columns. The stress-strain curve is linearly elastic up to about 30% of the maximum compressive strength. Above this point, the stress increases gradually up to the maximum compressive strength, f_{cu}, after that the curve descends into softening region, and eventually crushing failure occurs at an ultimate strain. The input data for the concrete, GFRP, and steel (high grade and mild steel) properties are shown in Table 2.

Table 2. Input data for the concrete, GFRP, and steel (main steel and stirrups) properties

	Concrete	GFRP	Steel (Main Reinf.)	Steel (Stirrups)
Unit weight N/mm^3	2.4e-5	2.54e-5	7.85e-5	7.85e-5
Ultimate compressive strength N/mm^2	25, 30, and 35	--	--	--
Tensile strength N/mm^2	1.8, 2.20, 2.50	460	415	240
Elastic modulus N/mm^2	2.2e4, 2.4e4, 2.6e4	4.4e4	2.5e5	2.5e5
Poisson ratio	0.20	0.20	0.30	0.30
Shear modulus N/mm^2	9.16e3, 10e3, 10.8e3	--	--	--

7. Loading and Nonlinear Solution

The analytical investigation carried out here is conducted on 10- RC columns; all columns are raised in vertical position with vertical load on the top surface. At a plane of support location, the degrees of freedom for all the nodes of the solid65 elements were held at zero. In a nonlinear analysis, the load applied to a finite element model is divided into a series of load increments

called load step. At the completion of each load increment, the stiffness matrix of the model is adjusted to reflect the nonlinear changes in the structural stiffness before proceeding to the next load increment. The ANSYS program uses Newton-Raphson equilibrium iterations for updating the model stiffness. For the nonlinear analysis, automatic stepping in ANSYS program predicts and controls the load step size. The maximum and minimum load step sizes are required for the automatic time stepping.

The simplified stress-strain curve for column model is constructed from six points connected by straight lines. The curve starts at zero stress and strain. Point No. 1, at $0.3f'_c$ is calculated for the stress-strain relationship of the concrete in the linear range. Point Nos. 2, 3 and 4 are obtained from Equation (9), in which $\varepsilon_{\square}$ is calculated from Equation (10). Point No. 5 is at ε_0 and f'_c. In this study, an assumption was made of perfectly plastic behavior after Point No. 5 (William and Warnke, 1975; Safari Gorji, 2009).

$$f = \frac{E_c \varepsilon}{1 + \left(\frac{\varepsilon}{\varepsilon_o}\right)^2} \tag{9}$$

$$\varepsilon_o = \frac{2 f_c^{/}}{E_c} \tag{10}$$

$$E_c = \frac{f}{\varepsilon} \tag{11}$$

Figure 3 shows the simplified compressive axial stress-strain relationship that was used in this study

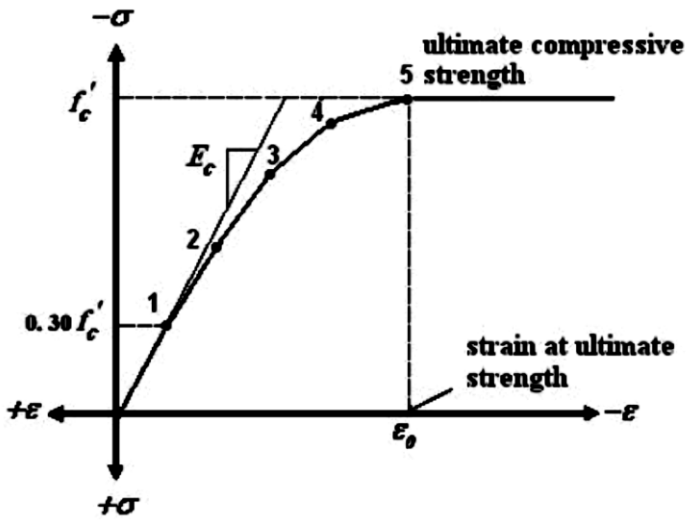

Figure 3. Simplified compressive axial stress-strain curve for concrete

8. Inelastic Analysis Results and Discussion

The parametric studies included in this investigation are the main reinforcement ratios and types, the transverse reinforcement ratios, and the characteristic strength of concrete, respectively. Table 3 shows the analytically results of the ultimate loads, deformations and compressive stress of concrete, respectively.

Table 3. Theoretical results of tested columns specimens

group No.	col. No.	dim (mm)		f_{cu} (N/mm^2)	Concrete stress N/mm^2	P_u (KN)	Def. (mm)
		dim	L				
	C1	250*250	1250	25	18	790	0.72
1	C2			25	20.5	900	0.79
	C3			25	21.1	935	0.83
2	C4			25	22.2	970	0.88
3	C5			30	26.4	940	0.78
	C6			35	32	1185	0.92
4	C7			25	21.5	870	0.82
	C8			25	22.27	955	0.85
5	C9			25	21.1	925	0.83
	C10			25	21.8	962	0.86

9. Experimental Validation

The validity of the proposed analytical model is checked through extensive comparisons between analytical and experimental results of RC columns under compression load. Figure 4 shows the theoretical and experimental load-deformation curve of tested columns from C1 to C8. The theoretical results from Finite Element Analysis showed in general a good agreement with the experimental values.

10. The Main Reinforcement Ratios

Figure 5 shows the theoretical load-deformation of columns C1, C2, C9, C3 and C10 which reinforced by GFRP reinforcement 4#12mm, 6#12mm, 4#16mm, 8#12mm and 4#18mm (0.723, 1.08, 1,286, 1.45 and 1.628 %) respectively; increasing GFRP reinforcement ratio leads to an increase in toughness and ductility of tested columns.

From Table 3, it can be seen that, ultimate loads, and ultimate strain C2, C9, C3 and C10 to C1 are (114,117,118&122%), and (109,115,115&119%) respectively. The increasing of main reinforcement ratios with GFRP bars increase the ductility of cross section, so it has a significant effect on ultimate strain, and ultimate loads that the columns resist.

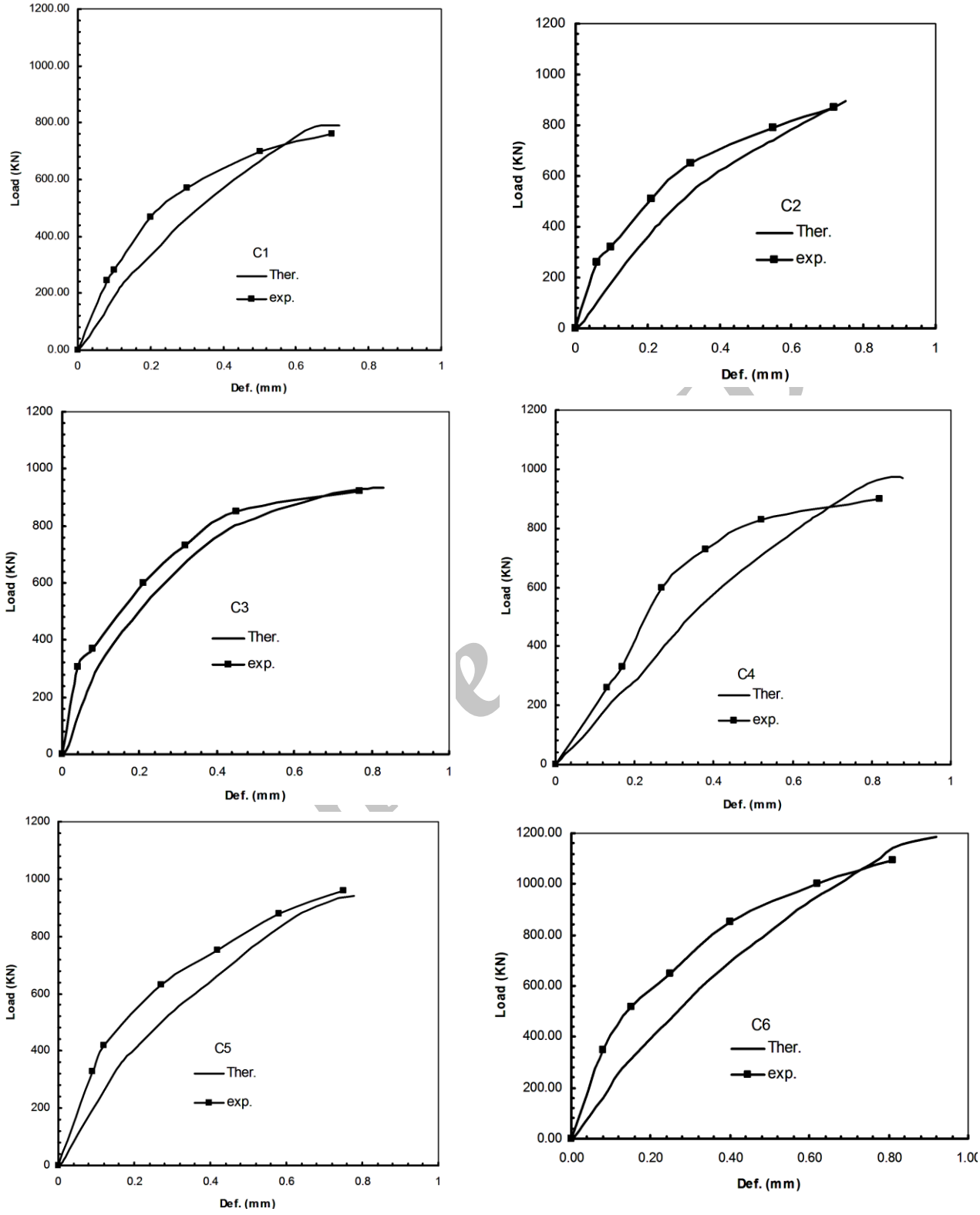

Figure 4. The theoretical and experimental load-deformation curve of tested columns from C1 to C8

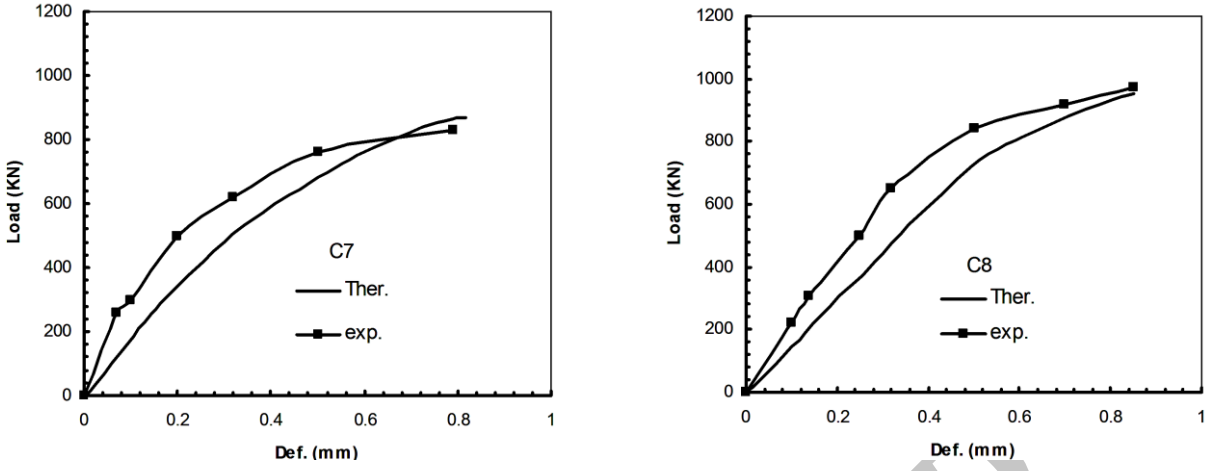

Figure 4 (Continue). The theoretical and experimental load-deformation curve of tested columns from C1 to C8

Figure 6 shows the effect of the main reinforcement ratios on the ultimate load that the columns resists, where the increasing of main reinforcement ratios from 0.723 to 1.2% has a significant effect on ultimate loads more than ratio from 1.2 to 1.62%.

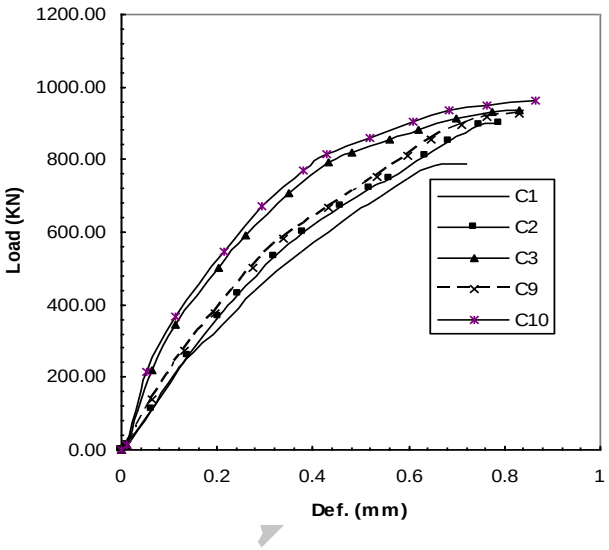

Figure 5. Load – deformation of C1, C2, C9, C3 and C10

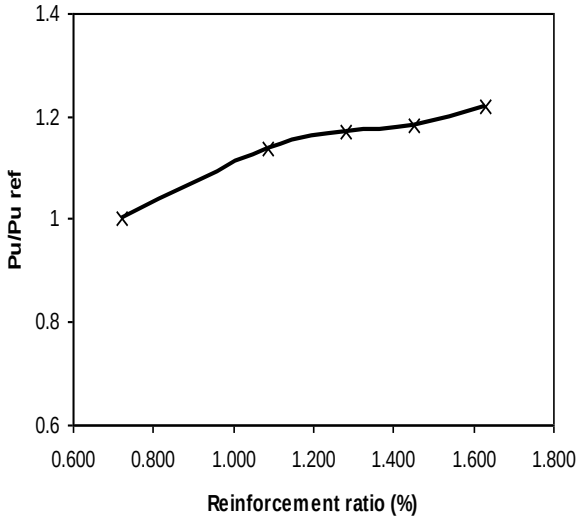

Figure 6. Ultimate Load of C2, C9, C3 and C10 to C1 and main reinforcement ratio

11. The Main Reinforcement Types

Figure 7 shows the load-deformation of columns C1 and C4 which reinforced by GFRP and steel reinforcement with 4#12mm (0.723%); tested column with steel reinforcement has ductility more than that in the column with GFRP reinforcement.

From Table 3, it can be seen that, ultimate load, and ultimate strain of C4 to C1 is 122.7 and 122.2 % respectively. Using steel as main reinforcement has a significant effect on the ultimate strain, and ultimate loads that the columns resist.

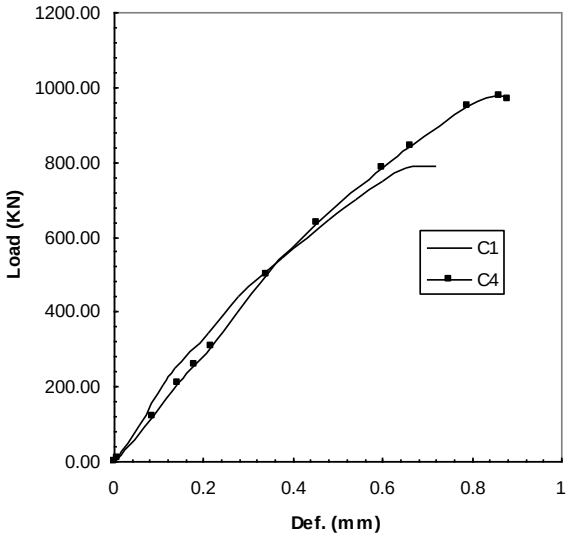

Figure 7. Load – deformation of C1 and C4

12. The Transverse Reinforcement Ratios

Figure 8 shows the load-deformation of columns C1, C7 and C8; increasing of transverse reinforcement ratio leads to an increase in toughness and ductility of tested columns. From Table 3, it can be seen that, ultimate loads, and ultimate strain of C7 and C8 to C1 are (110 &120 %) and (113&118 %) respectively.

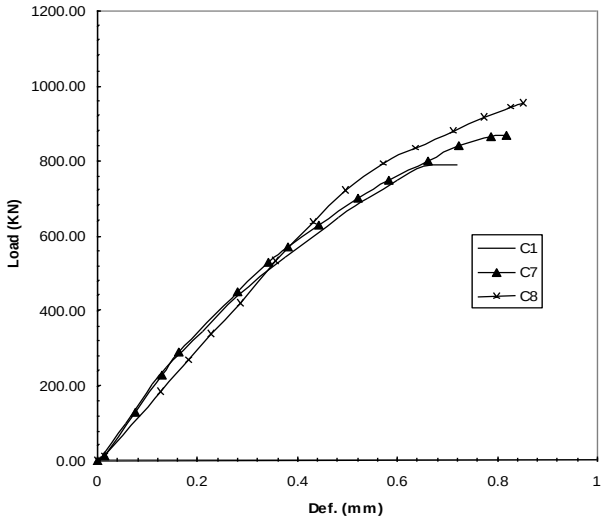

Figure 8. Load–deformation of C1, C7 and C8

Figure 9 shows the effect of the transverse reinforcement ratios in the column ends on the ultimate load that the columns resists, where the increasing of transverse reinforcement ratios has a significant effect on ultimate loads. The increasing of transverse reinforcement ratios confines the columns so it is lead to an increase in the ultimate loads and increasing ultimate strain.

As the increasing of transverse reinforcement ratio leads to an increase in toughness and ductility of tested columns with GFRP, so it will be compared to the tested column with steel reinforcement and normal stirrups distribution. It can be seen that, ultimate loads, and ultimate strain of C4, C7 and C8 to C1 are (122, 110 &120 %), and (122, 113&118 %) respectively.

Figure 10 shows the load-deformation of columns C1, C7, C8 and C4, increasing stirrups with columns reinforced by GFRP increases the toughness and ductility of columns more than using steel bars with normal stirrups distribution, the behavior of column with steel bars C4 generate between the behaviors of C7 and C8.

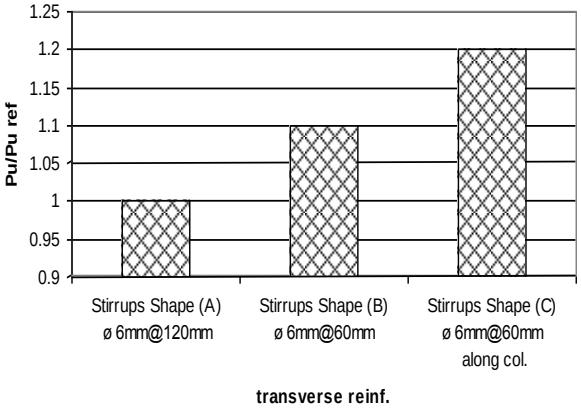

Figure 9. Ultimate Load of C1, C7 and C8 and transverse reinforcement

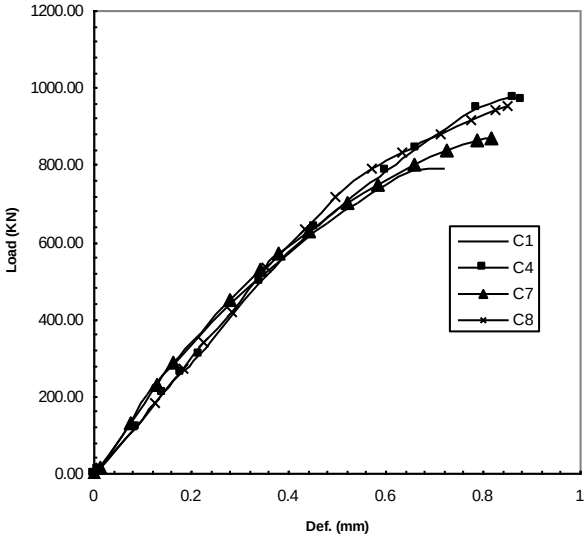

Figure 10. Load – deformation of C1, C4, C7 and C8

12.1. The Characteristic Compressive Strength of Concrete

From Table 3, it can be seen that, ultimate loads, and ultimate strain of C5 and C6 to C1 with (25, 30 &35N/mm^2) are (119 &150 %) and (108&128%) respectively. Figure 11 shows the load-deformation of columns C1, C5 and C6; increasing the characteristic strength of concrete has a significant effect on the behavior of tested columns that increases toughness and ductility of tested columns.

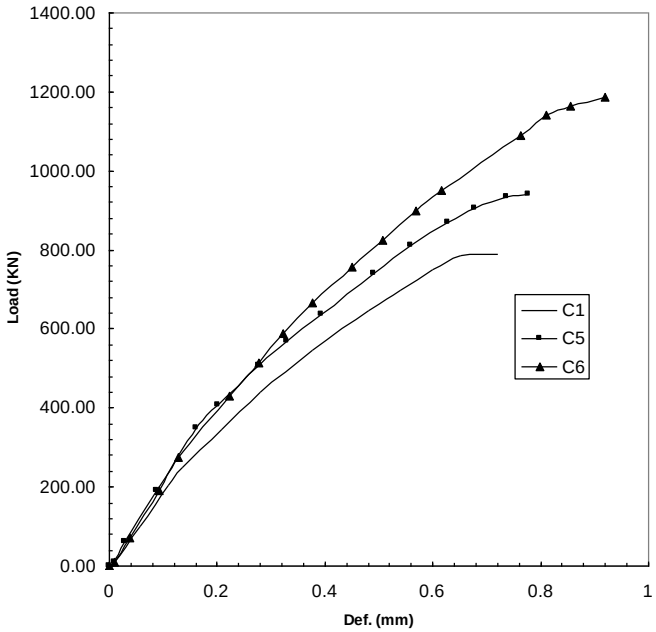

Figure 11. Load–deformation of C1, C5, C6

Figure 12 shows the effect of the characteristic strength of concrete on the ultimate load that the columns resists, where the increasing of characteristic strength of concrete has a significant effect on ultimate loads.

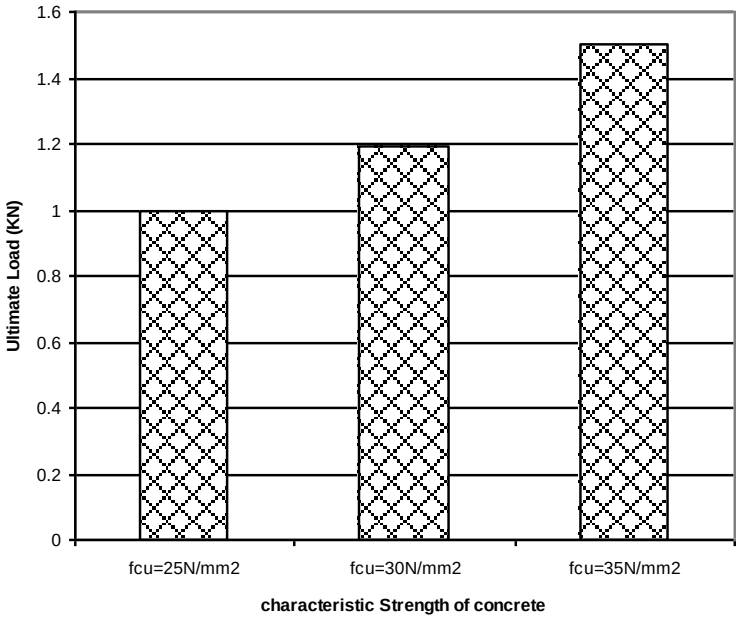

Figure 12. Ultimate Load of C1, C5 and C6 and characteristic strength of concrete

13. Predicted Formula

Unfortunately, there was lack of data about using FRP as reinforcement; lack of a comprehensive database on FRP materials makes it difficult for the practicing civil engineers and designers to use FRP composites on a routine basis, although a number of reviews have been published recently related to durability and test methods.

The focus of each has been to summarize the state of knowledge in general without emphasizing or attempting to prioritize critical areas in which needs are the greatest for collection, assimilation, and dissemination of data (Karbhari et al., 2003).

Different formulas were used to predict a general formula to calculate the maximum applied load for tested columns reinforced by GFRP as the main reinforcement; Table 4 shows applied Load (KN), by using formulas.

Table 4. Applied Load (KN), by using different formulas

No	Col	Dim (mm)		F_{cu} (KN)	Reinf Ratio (%)	Applied Load (KN)					
		Dim	L			Exp. Data[1]	(ACI-318-08)[2]	(Egyptian Code)[3]	(BS 8110)[4]	Finite Element (ANSYS)[5]	Predicted formula
1	C1	250*250	1250	25	0.723	760	758	686	791	790	781
2	C2			25	1.08	870	818	756	875	900	859
3	C3			25	1.45	920	878	825	958	935	937
4	C5			30	0.723	960	884	796	916	940	902
5	C6			35	0.723	1095	1011	905	1041	1185	976
6	C9			25	1.286	--	851	795	921	925	906
7	C10			25	1.628	--	908	860	999	962	1031

(1) Experimental Results of tested specimens, (2) American Concrete Institute (ACI) Committee 318 (American Concrete Institute, 2008), (3) Egyptian Code for design and construction of concrete structures (2001), (4) British Standards Institution (BSI), (5) Numerical Finite Element (ANSYS).

Figure 13 shows the relation between applied load and reinforcement ratio by previous methods, and explains also the predicted formula to calculate the maximum applied load for tested columns reinforced by GFRP as main reinforcement.

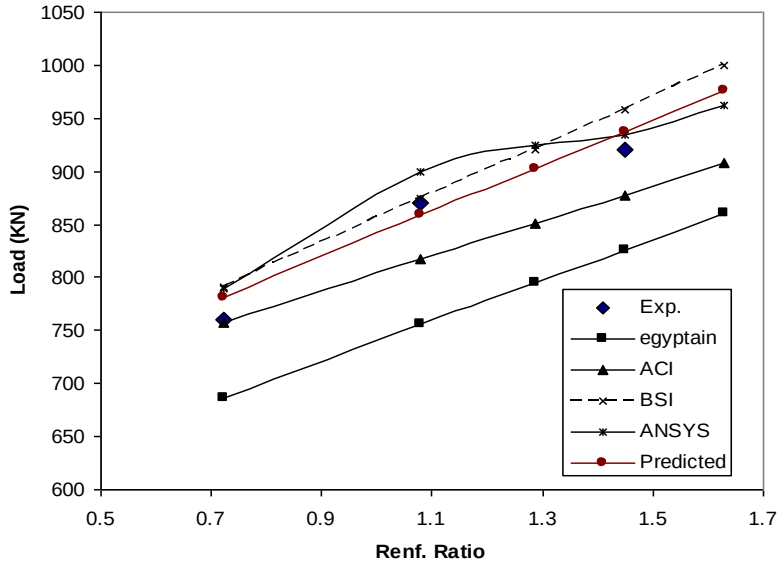

Figure 13. Relationship between applied load and flexural reinforcement ratio

By using the previous formula to draw the relationship between the reinforcement ratio and the maximum normal forces of the mentioned sections in the following Table, which are used, and comparing those results with the experimental applied forces. Hence a new general formula was predicted from the experimental data, which was the average of data, as follows:

$$N = 0.4 f_{cu} A_c + 0.75 f_y A_s \tag{12}$$

Where:

N= axial load capacity of the reinforced concrete column with GFRP

f_y = Yield strength of FRP

A_c= Cross section Area of concrete

A_{sc}= Cross section area or main reinforcement

f_{cu} = Ultimate compressive strength of the concrete

14. Summary and Conclusions

The inelastic behavior of 10 columns are investigated in the current study under the effect of increasing loading employing the inelastic FE analysis program ANSYS. Several parameters are investigated including the main reinforcement ratios, the main reinforcement types, the transverse reinforcement ratios, and the characteristic strength of the concrete. The study focuses on the consequences of the investigated parameters on the deformation and ultimate resisting load. The conclusions made from this investigation are:

1-The theoretical results from Finite Element Analysis showed in general a good agreement with the experimental values

2-Increasing GFRP reinforcement ratio leads to an increase in toughness and ductility of tested columns.

3-Increasing GFRP reinforcement ratio has a significant effect on ultimate loads.

4-Increasing GFRP reinforcement ratio from 0.723 to 1.2% has a significant effect on ultimate loads more than ratio from 1.2 to 1.628%

5-Tested column with steel reinforcement has ductility more than the column with GFRP reinforcement.

6- Increasing of transverse reinforcement ratios in columns reinforced by GFRP bars increases toughness and ductility of columns more than using steel bars with normal stirrups distribution.

7-Increasing of characteristic strength of concrete has a significant effect on the behavior of tested columns reinforced by GFRP bars where it increases toughness and ductility of tested columns.

8- A new general formula was predicted from the experimental data, which was the average of data, as follows:

$$N = 0.4 f_{cu} A_c + 0.75 f_y A_s \tag{13}$$

Where:

N= axial load capacity of the reinforced concrete column with GFRP

f_y = Yield strength of FRP

A_c= Cross section Area of concrete

A_{sc}= Cross section area or main reinforcement

f_{cu}= Ultimate compressive strength of the concrete

References

ACI Committee 440 (2006), "Guide for the design and construction of structural concrete reinforced with FRP bars", ACI 440.1R-06, *American Concrete Institute*, Farmington Hills, MI., USA.

American Concrete Institute (2008), "Building code requirements for structural concrete", ACI 318-08, *American Concrete Institute*, Farmington Hills, MI., USA.

ANSYS User's Manual (1995), Swanson Analysis Systems, Inc., USA.

British Standards Institution (BSI). (1997), "Structural use of concrete' Part 1: Code of practice for design and construction", BS8110-1:1997, London, UK.

Choo, C.C., Harik, I. E. and Gesund, H. (2006), "Minimum reinforcement ratio for fiber-reinforced polymer reinforced concrete rectangular columns", *ACI Structural Journal*, Vol. 103, May-June, Pages 460-466.

Egyptian Code for Design and Construction of Concrete Structures, Code No. 203, 2001.

EL-Salakawy, E.F., Kassem, C. and Benmokrane, B. (2003), "Construction, testing and monitoring of FRP reinforced concrete bridges in North America", *NSERC Chair, ISIS Canada*, Department of Civil Engineering, Université de Sherbrooke, *Sherbrooke*, QB, Canada.

Halcrow, W. and Partners Ltd; London, England, (1996), "FRP Concrete Structures", *Advanced Composite Materials in Bridges and Structures*, *Canadian Society for Civil Engineering*, Montreal, QB., Canada.

Karbhari, V.M., Chin, J.W., Hunston, D., Benmokrane, B., Juska, T., Morgan, R., Lesko, J.J., Sorathia, U. and Reynaud, D. (2003), "Durability gap analysis for fiber-reinforced polymer composites in civil infrastructures", *Journal of Composites for Construction, ASCE*, Vol. 7, No. 3, Pages 238-247.

Nicholas, M. and Rajan, S. (2003), "The fatigue of fiber-reinforced polymer composite structures state-of-the-art review", Civil and Environmental Engineering, *University of South Florida, College of Engineering*, Tampa, FL., USA.

OU, J. and LI, H. (2003), "Recent Advances of Structural Health Monitoring in Mainland China", *The National Hi-Tech Research and Development Program (HTRDP), and practical engineering projects*, China.

Safari Gorji, M. (2009), "Analysis of FRP strengthened reinforced concrete beams using energy variation method", *World Applied Sciences Journal*, Vol. 6, No. 1, Pages 105-111.

William, K.J. and Warnke, E.D. (1975), "Constitutive model for the triaxial behavior of concrete", *Proceedings of the International Association for Bridge and Structural Engineering*.

Zienkiewics, D.C. (1967), "The Finite Element Method in Structural and Continuum Mechanics", *McGraw-Hill*, London, UK.